Available online at www.CivileJournal.org

Civil Engineering Journal

(E-ISSN: 2476-3055; ISSN: 2676-6957)

Vol. 11, No. 01, January, 2025

Experimental Investigation of Single and Intermittent Light Non-Aqueous Phase Liquid Spills Under Dynamic Groundwater

Doaa F. Almaliki [1, 2], Harris Ramli [1*], Ali Zaiter [1]

[1] School of Civil Engineering, Engineering Campus, Universiti Sains Malaysia, 14300 Nibong Tebal, Pulau Pinang, Malaysia.

[2] Environment and Pollution Engineering Department, Basrah Engineering Technical College, Southern Technical University, Basrah, Iraq.

Received 04 October 2024; Revised 18 December 2024; Accepted 25 December 2024; Published 01 January 2025

Abstract

The groundwater contamination from petroleum by-products represented in Light Non-Aqueous Liquid (LNAPL) under groundwater table fluctuations has become a serious environmental problem. For this reason, developing a rapid response strategy incorporating experimental characterization of LNAPL distribution trajectories is crucial for assessing the threats of LNAPL contaminants in the subsurface environment. In this study, the influence of various LNAPL spills in a porous medium under dynamic groundwater conditions was investigated using the Simplified Image Analysis Method (SIAM). Single and intermittent LNAPL (diesel) spills of total volume (400 and 800 ml) were examined in a river sand two-dimensional tank (70 cm × 70 cm × 3.5 cm) under the effect of groundwater table fluctuation. The results indicated that the contaminant was distributed above h=28 cm in the 400 ml LNAPL spill. However, it migrated below h=28 cm, and its saturation reached 36% when the LNAPL volume raised to 800 ml. The LNAPL saturation in the case of four LNAPL intermittent spills was more evenly distributed through the tank depth than in the cases of a single spill of 800 ml and two intermittent spills of 400 ml. Furthermore, LNAPL migrated to a larger depth in the system (h=18.5 cm) only in the case of four LNAPL intermittent spills and under groundwater table fluctuation, which poses a significant threat to the groundwater. This study highlights the importance of the effect of various LNAPL spills under dynamic groundwater conditions, which can offer valuable guidance for developing remediation schemes.

Keywords: LNAPLs; Repetitive Spills; Diesel; Groundwater Table Fluctuation; Saturation; Migration.

1. Introduction

Groundwater and soil have become increasingly contaminated by organic pollutants and their by-products present in Light Non-Aqueous Phase Liquids (LNAPLs) form due to the seepage resulting from mining, processing, and transportation operations. LNAPLs have been identified as a significant environmental problem that requires a fast response to be resolved [1-3]. These pollutants have adverse impacts on the quality of groundwater, making it inappropriate for human consumption and irrigation [4-6]. Even minimal exposure to LNAPL contaminants can pose significant risks to human health and ecological hazards to the environment [7-10]. Due to their low aqueous solubility, certain LNAPLs can persist in water for a long period. This creates long-term sources of contamination for soil and groundwater, which has become a common and challenging problem to control [11-13]. When the LNAPL is released, it migrates downward into the saturated zone forming a pool of contaminants due to the effect of gravity, leaving some portions of residual ganglia in the unsaturated zone [14, 15]. If the LNAPL is spilled in sufficient volume, it can form zones with complicated LNAPL interaction and composition due to overlapped contamination. Therefore, understanding the migration of LNAPL in the subsurface environment is crucial for evaluating the contamination source zones and implementing efficient remediation measures.

* Corresponding author: cemhr@usm.my

http://dx.doi.org/10.28991/CEJ-2025-011-01-017

Groundwater table fluctuation (GWTF) significantly influences the distribution of LNAPL in the subsurface environment. Groundwater table fluctuation in hydrological systems changes due to groundwater recharge, exploitation, tidal activities in coastal regions, rainfall infiltration, water fluctuations of lakes and rivers, and seasonal variations in the surrounding water bodies, which in turn produce distinctive features resulting from the wetting and drying cycles influencing differences in soil water content, redox circumstances, and biogeochemical characteristics [16-19]. Fluctuations in the groundwater can lead to the entrapment of LNAPL beneath the water table. This will establish a new equilibrium, leading to a more intricate process of pollutant transportation [20-22]. Moreover, the spatial distribution of LNAPLs within an aquifer is influenced by variations in the elevation of the water table, particularly in the vertical direction. When the capillary fringe and water table drop, LNAPLs move downward with the flowing water, leaving residual portions of LNAPL in the unsaturated zone [23-25]. Furthermore, the subsequent increase in the groundwater table forces part of the LNAPL to migrate upwards in the opposite direction [26], resulting in trapped LNAPL beneath the water table [27]. This can threaten groundwater resources for long periods, while traditional techniques may be inadequate for remediation. Hence, understanding the movement of the LNAPLs under dynamic groundwater conditions is crucial for assessing the contamination and the development of remediation strategies [28, 29].

In previous studies, the interaction of LNAPL migration with groundwater table fluctuation has been investigated experimentally. Driven by the severe environmental risks of LNAPL leakage, Shen et al. [30] investigated experimentally the LNAPL migration in fractures filled with sand. Results showed that as the sand permeability increased, the migration velocity increased. During groundwater table fluctuation, LNAPL migrated downward through the drainage stage and was entrapped in the imbibition stage. Their findings revealed a large, significant effect of the fracture inclination on the LNAPL migration velocity, where lower fracture inclination showed reduced migration velocity and vice versa. In the study of Alazaiza et al. [31], a two-dimensional (2D) tank with a double porosity soil structure was used to evaluate the LNAPL movement under different rainfall intensities. The results showed that LNAPL was entrapped in porous media due to water table fluctuation. Moreover, the LNAPL volume and rainfall infiltration directly affected the height of the capillary fringe. The effect of the drainage and imbibition cycles of groundwater table fluctuation on LNAPL redistribution was investigated in the study of Yimsiri et al. [32] with the aid of the Simplified Image Analysis Method (SIAM). Results showed that the LNAPL vertical diffusion and mass transfer are amplified with groundwater table fluctuation. Groundwater table fluctuation, whether due to seasonal changes or pump-induced, produces continuous LNAPL redistribution during the different phases (free, trapped, and residual) and consequently increases the release of hydrocarbons to the vapor and dissolved phases and enhances the pollution biodegradability [33].

The LNAPL passage in the subsurface layers depends on several factors, such as the volume of the spilled LNAPL. The LNAPL distribution due to groundwater fluctuation is investigated experimentally in a one-dimensional (1D) square column in the study of Alazaiza et al. [34] by testing two LNAPL volumes of 25 ml and 50 ml with the aid of the SIAM. The water level fluctuated between 18 and 28 cm high during the drainage-imbibition cycles. It is reported that for higher LNAPL volume, LNAPL covered a larger extent and pushed the water downwards to reach deeper depths. Yet, the changes in LNAPL volume under the same groundwater cycles did not change the overall behavior of LNAPL pushing the water downwards to occupy the soil pores. In the studies of Flores et al. [35] and Azimi et al. [36], LNAPL distribution and saturation under the same fluctuation pattern due to different LNAPL viscosity and grain sizes were investigated methodically. They focused in their works on the variations of LNAPL distribution and saturation under the effect of changes in groundwater table fluctuation. Alazaiza et al. [37] conducted experimental tests in a 1D rectangular column filled with natural river sand and injected with three LNAPL volumes of 50, 100, and 150 ml to understand the effect of LNAPL volume on the contamination distribution and migration through the capillary fringe. However, this study did not consider the effect of groundwater table fluctuation as the water level was set at 29 cm high from the column bottom through the experiments. The SIAM technique was used for visualizing and analyzing the LNAPL behavior. The results showed that LNAPL migrated faster and into deeper extents as the injected LNAPL volume increased. This is attributed to the relatively higher pressure and gravitational force associated with larger LNAPL volumes, which, at a certain threshold, can overcome the capillary force resulting from the interaction between the water molecules and the sand surface. Despite the injected LNAPL volume, LNAPL showed fast migration in the first few minutes of the experiments before the migration velocity started to drop gradually. This velocity pattern is due to the pressure exerted by LNAPL to migrate through the sand voids. To improve LNAPL remediation and treatment strategies through understanding the LNAPL behavior in the contaminated areas, Lenhard et al. [38] developed an analytical approach to predict the LNAPL distribution of three phases (free, residual, and entrapped) and the vadose zone through the current and historic recorded water levels of wells. Two hypothetical porous media (clay loam and loamy sand) were in for understanding the effect of water fluctuation on LNAPL transmissivity. To improve the efficiency of remediation techniques, a deep understanding of the LNAPL behavior and characteristics through porous media with dynamic conditions is required.

Recently, Zheng et al. [39] studied the LNAPL (benzene and toluene) behavior in single- and double-lithology soil columns under dynamic conditions. The LNAPL migration was significantly affected by flushing hydraulic forces induced by water fluctuation. On the other hand, the LNAPL was mainly affected by retention resulting from the 10 cm of silt of high adsorption in the case of double lithology soil columns. Moreover, LNAPL dissolution was correlated with LNAPL migration in the saturated zone, and LNAPL saturation dropped as the water level rose and vice versa. The aforementioned study recommended a double lithology soil matrix to ease LNAPL removal from the silt layer, whereas LNAPL contamination of single lithology soil requires additional efforts within the groundwater. These investigations improve our comprehension of the redistribution characteristics of LNAPL under fluctuating water tables. However, there is still a lack of studying the effect of repetitive LNAPL spills on LNAPL distribution behavior when the system is subjected to groundwater table fluctuations.

Repetitive LNAPL spills can occur due to certain factors like industrial operations, infrastructure matters, and operational activities. Moreover, operational activities play a significant role with other factors such as poor training, insufficient maintenance, human mistakes, or failure to apply standard practices adopted for recurring incidents, which can elevate the threats of repetitive LNAPL contamination. Furthermore, external factors (extreme weather or logistic accidents) can also increase the risk of repetitive LNAPL spills, making it crucial for industries to follow mitigation measures and robust monitoring systems to reduce repetitive spills. The repetitive LNAPL spills can lead to significant contamination of soil and groundwater. It can pose high risks to groundwater resources and damage agricultural life. Focusing on the effect of repetitive LNAPL spills helps in understanding the cumulative effects of LNAPL and its potential risks to human health. This helps in designing cleanup strategies and minimizing the risk of environmental damage. Previous studies reported significant findings on LNAPL movement and fate through porous media and investigated the effect of LNAPL volume, soil particle size, and groundwater table fluctuation on LNAPL migration behavior through porous media. Yet, there are some limits, such as the case of Alazaiza et al. [37], where the effect of LNAPL volume is tested but under static water conditions. The elucidation of the subsurface LNAPL movement and saturation under groundwater table fluctuation is fairly complicated. Up-to-date, the effect of repetitive LNAPL spills mimicked by repetitive LNAPL injections under dynamic conditions has not been studied yet. This study aims to extend the acquired knowledge on LNAPL behavior beyond those that have been studied experimentally by presenting the first experimental approach to understanding the LNAPL behavior under repetitive injections with groundwater table fluctuation. A two-dimensional tank is filled with natural river sand and subjected to single and repetitive LNAPL injections for volumes of 200, 400, and 800 ml. The non-invasive dynamic Simplified Impact Analysis Method (SIAM) is adopted to visualize and quantify the changes in LNAPL characteristics through experiments.

2. Materials and Methods

2.1. Material Characteristics

Natural river sand was collected and utilized as the porous medium in the current study. Before conducting the experiments, the sand properties were examined initially through initial characterization. The conducted particle size analysis revealed that the pore grain size ranged from 2 mm to 0.15 mm, with an average grain size of 0.7 mm. The physical properties of the sand are summarized in Table 1. Diesel was selected as LNAPL in this study as it is a common LNAPL contaminant existing in the subsurface environment with a density of 0.83 g/cm³ and a viscosity of 5.8 mm²/s at 20°C. To improve the visual observation of the LNAPL and enhance the light absorption through running the experiments, it was necessary to dye the LNAPL using Red Sudan III dye. De-aired water was used to saturate the sand in all the research experiments. For more visual observation, the de-aired water was dyed using Acid Blue 9 dye. The dilution factor for preparing the red and blue dyed liquids was 1:10,000 as described by Ramli [28].

Table 1. Sand physical characteristics

Properties	Parameter	Unit	River Sand
Textural composition	Gravel	%	24.04
	Sand	%	75.65
	Fines	%	0.31
	D_{10}	mm	0.36
	D_{30}	mm	0.85
	D_{50}	mm	1.43
	C_u	-	4.90
	C_c	-	1.13
Moisture content	M_c	%	6.52
Density	Specific gravity	G_s	2.635
Hydraulic conductivity	K_{sat}	cm/s	0.135

D_{10}, D_{30} and D_{50}: diameter where 10%, 30% and 50% of soil are finer (mm), respectively; C_u: coefficient of soil uniformity and C_c: coefficient of curvature.

2.2. Experimental Setup

All the experiments were conducted in a two-dimensional (2D) tank to investigate the LNAPL migration behavior under the influence of various LNAPL spills when the system is subjected to groundwater table fluctuation. A schematic diagram of the experimental setup is shown in Figure 1. The experimental devices include the 2D tank apparatus, the LNAPL injection system, the water table control part, and the SIAM system. The 2D tank employed in this study was fabricated from 10 mm thick transparent acrylic material to enhance visual observation through the tank walls. The 2D tank was divided into the porous media chamber and the-sided spacers. The sand was filled in the porous media section of 60 cm in length, 70 cm in height, and 3.5 cm in width. To enhance the clarity of the groundwater level inside the tank, two spacers fabricated from acrylic material measuring 4 cm in length, 3.5 cm in width, and 70 cm in height were installed into the tank on both sides. To ensure free water flow and prevent valve blockage by soil particles, each spacer was sealed with a 150 μm-opening nylon mesh sheet.

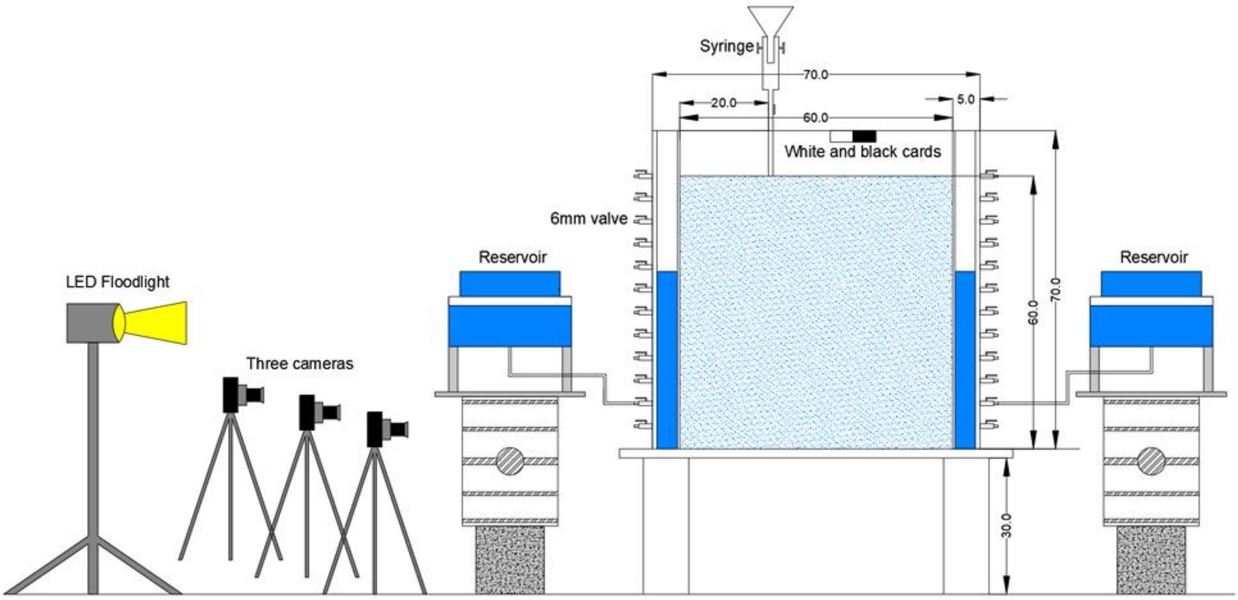

Figure 1. Schematic setup of a 2D tank with a water circulation system (all dimensions are in centimeters)

The water flow in the conducted tests was constant where there is no hydraulic flow gradient to consider below the groundwater table. Two reservoirs were placed on a jack on the left and right sides of the tank to create an adjustable water level setup as shown in Figure 1. Each reservoir was connected to either the inlet or the outlet valve via a transparent PVC pipe of 6 mm in diameter. The water circulation system was constructed to replicate the asymmetrical movement of the groundwater table at the intended water level. During water table fluctuation, the reservoirs were raised and lowered to the desired height. In all the experiments, the main water table height before diesel injection was set at h=28 cm high. The height (h) level in this study refers to the height from the tank bottom, which is considered the reference level. The LNAPL (diesel) was injected using an 800 ml graduated syringe connected to a 10 cm in length and 0.6 cm in diameter tube and positioned at the top of the tank using a support stand. The LNAPL injection syringe was located 21 cm from the left side of the tank and 4 cm deep inside the porous media to provide a simple, well-defined release and avoid the upward movement of LNAPL during the injection.

Due to the cost-effectiveness and accuracy, the SIAM technique measures the LNAPL and water saturation in the 2D flow tank [40, 41]. The SIAM system was mainly composed of three Nikon D5300 cameras for collecting images and storing them for the next stage of image processing and LED floodlight. Two camera lenses were connected to two different bandpass filters with 470 nm and 650 nm wavelengths to read the water and LNAPL saturation, respectively. The third camera was set to be the control camera without any bandpass filter to capture natural images for the experimental system. The cameras were connected to three computers and controlled using the Nikon Camera Control Pro 2 application. The aperture settings of the two lenses were modified using exposure periods of a few seconds to fully use the camera's dynamic range. The lenses' apertures were set to f-3.5, and the shutter speed was 1/6 seconds for all of the collected images. The digital cameras were placed in a fixed position of 2 m from the flow chamber and set to take images automatically every 30 minutes. An LED floodlight was installed next to the cameras in a dark room to provide consistent lighting on the tank. All the experiments were conducted at a temperature of 25℃ ± 1℃.

The experimental arrangements of various LNAPL spills are illustrated in Figure 2. Where the alphabet R denotes the (repetitive) case and the number following the R refers to the number of LNAPL injection stages. The LNAPL volume of 400 ml was spilled in one single injection (400R1) and repetitive injections (two spills each of 200 ml), as in the case of 200R2. The total of 800 ml LNAPL volume was injected in four intermittent injections (200 ml each injection) as in the case of 200R4, two intermittent injections (400 ml each spill) as in the case of 400R2, and 800 ml in one single injection as in the case of 800R1. Two cycles of water table fluctuations (drainage/imbibition) were applied after each LNAPL injection stage.

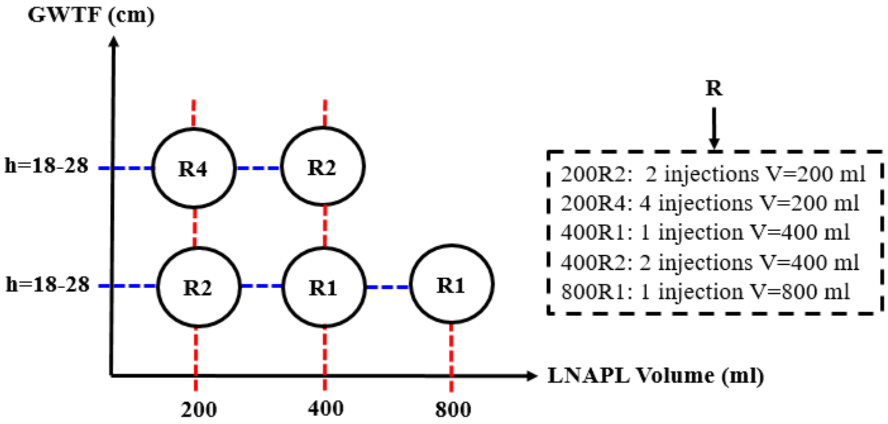

Figure 2. Experimental arrangements of single and repetitive LNAPL spills

2.3. Experimental Procedures

The initial step in the experimental procedure was to fill the tank with the porous medium gradually and slowly until the height of h=60 cm. To ensure uniform sand backing, reduce the trapped air bubbles in the tank, and produce uniform density in the entire domain, a 5 cm height of the prepared blue-dyed water was first introduced into the 2D tank. Then saturated sand with blue-dyed water was poured from the top of the tank using a small spoon incrementally in 5 cm per layer until the height of 60 cm from the tank bottom. All the experiments were started when the bottom tank valves on both sides opened and the water saturating the soil drained due to the effect of the gravitational force. In all the experiments, the water table height before LNAPL injection was fixed to be at h=28 cm. At t=21 hr, the diesel was slowly and cautiously injected into the medium through the syringe. To investigate the effect of single and repetitive spills of LNAPL on water and LNAPL saturation and distribution under the effect of groundwater table fluctuations, two different LNAPL volumes were compared (400 and 800 ml). The time-dependent water table fluctuations and volume-injected adjustments are presented in Figure 3. Two cycles of groundwater table fluctuation are conducted after each LNAPL injection stage. The alterations in groundwater table fluctuation (drainage and imbibition) are described as follows:

- The first drainage stage: the water level was decreased from h=60 cm to h=28 cm, by allowing water to exit the 2D tank through the drainage line over 9 hours.
- The second drainage stage: the water table was lowered by 10 cm from h=28 cm to h=18 cm by reducing the height of the external reservoirs on both sides of the tank to allow the water to drain out of the tank over 6 hours.
- The first imbibition stage: the water level within the tank was elevated by 10 cm from h=18 cm to h=28 cm, through the natural upward movement of water inside the tank. The tank was left undisturbed for 6 hours.
- The first LNAPL injection stage: LNAPL was injected through the graduated syringe fixed at the top of the tank and the tank was left for 12 hours for stabilization.
- The third drainage stage: the groundwater table was lowered from h=28 cm to h=18 cm. The stabilization time for this stage was 12 hours.
- The second imbibition stage: during this stage, the groundwater level is raised back to h=28 cm by fixing the external reservoir height on the level of 28 cm to allow the water to enter the system. The stabilization time for the system during the stage was 12 hours.
- The fourth drainage stage: after the second imbibition, the water level reduced again from h=28 cm to h=18 cm. The stabilization time for the system in this stage is 12 hours.
- The third imbibition stage: in this stage, the water increased back to h=28 cm. The time for this stage is 12 hours.

The second, third, and fourth LNAPL injection stages: in the case of repetitive LNAPL injections, the previous stages starting from the LNAPL injection stage to the third imbibition stage were repeated.

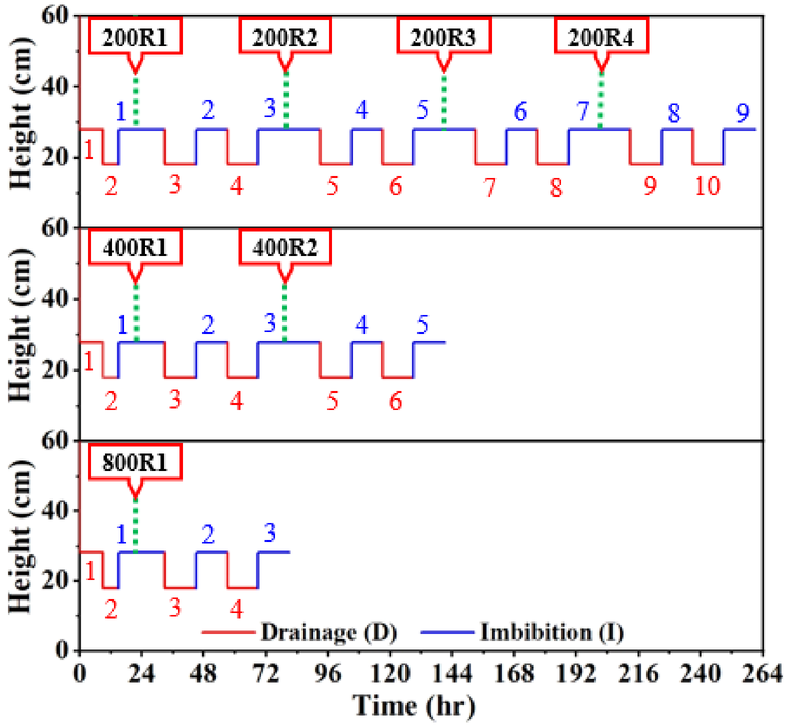

Figure 3. Time-dependent water table fluctuations and LNAPL volume-injected

2.4. The Principle of SIAM

Simplified Image Analysis Method (SIAM) is a non-invasive and non-destructive technique used to measure this study's LNAPL and water saturation. The method was developed by Flores et al. [40] to simplify the complexity of the calibration process of the Multispectral Image Analysis Method (MIAM). The theory underlying SIAM is based on the application of the Beer-Lambert equation of transmittance. This equation allows for the establishment of linear correlations between water saturation (S_w), LNAPL saturation (S_o) and average optical density. By utilizing these correlations, it becomes possible to estimate fluid saturations in porous media throughout the entire domain. This phenomenon is described by the Beer-Lambert Law of Transmittance [42]. The average of the optical density was determined using the following Equation:

$$D_i = \frac{1}{N}\sum_{j=1}^{N} d_{ji} = \frac{1}{N}\sum_{j=1}^{N}\left(-\log_{10}\left(\frac{I_{ji}^{r}}{I_{ji}^{o}}\right)\right) \tag{1}$$

where D_i is the average optical density, i represents the spectral band (i=470 nm or i=650 nm), N denotes the total number of pixels in the selected area of interest, d_{ji} is the optical density of the individual pixels for a given spectral band i, I_{ji}^{r} is the reflected light intensity, and I_{ji}^{0} denotes the intensity of light reflected by a brilliant white surface [43].

Water and LNAPL saturation can be estimated from the calculated D_i by conducting a comparison of the average of the optical densities' matrix elements and three calibration images (D^d_i, D^w_i, D^0_i) for dry sand (S_w= 0 %, S_o= 0 %), fully saturated sand with water (S_w=100 %, S_o=0 %) and fully saturated sand by LNAPL (S_w= 0 %, S_o= 100 %). Equation 2 demonstrates a matrix of correlation equation sets, with each one corresponding to each cell.

$$\left[\begin{pmatrix} D_i \\ D_j \end{pmatrix}_{m.n}\right] = \begin{bmatrix} (D_i^{10} - D_i^{00}) \cdot S_w + (D_i^{01} - D_i^{00}) \cdot S_o + D_i^{00} \\ (D_j^{10} - D_j^{00}) \cdot S_w + (D_j^{01} - D_j^{00}) \cdot S_o + D_j^{00} \end{bmatrix}_{m.n} \tag{2}$$

where m and n denote the matrix dimensions, $[D_i]_{mn}$ and $[D_j]_{mn}$ refer to the average optical density of each mesh element for wavelengths i and j, $[D_i^{00}]_{mn}$ and $[D_j^{00}]_{mn}$ represent the average optical density of each mesh element of dry sand, $[D_i^{10}]_{mn}$ and $[D_j^{10}]_{mn}$ mean the average of optical density of water-saturated sand, and $[D_i^{01}]_{mn}$ and $[D_j^{01}]_{mn}$ are the average of optical density for LNAPL saturated sand. The average optical densities of the three fluids (air, water and LNAPL), each represents by saturation.

2.5. Image Analysis

The SIAM technique is a non-invasive and non-intrusive method for determining fluid saturations over a wide area. The advantage of using SIAM is that it needs the least amount of equipment, is the cheapest, and produces no adverse radiation effects. It is a non-intrusive, non-destructive approach for measuring fluid saturations in a porous medium. The images captured were stored in the computer for image processing. First, the images were converted from NEF (Nikon

Electronic Format) to TIFF (Tagged Image File Format) using Nikon ViewNX2 software. Before analysing the captured images and removing the effect of light intensity changes, an image correction operation as proposed by Bob et al. [44] was applied to the captured images. The reference image was acquired when the 2D tank was fully saturated with water. According to Alazaiza et al. [34, 41], two small sections (8 cm x 8 cm) within the reference image were identified as "correction zones". Identifying "correction zones" was to ensure that these areas were completely saturated with water in every image. The ratio of the average light intensity of the correction zones in the reference image to the average light intensity of the correction zones in the image that required processing was used to calculate the correction coefficients. The corrected image was derived by multiplying the intensity of the image with the corresponding correction coefficient. Three consecutive frames were taken for every image, and the average light intensities of these three frames were utilized in the computations [37]. These corrected images were then used as the basis for a quantitative analysis of LNAPL saturation. Then, the TIFF images were analysed using MATLAB software. According to the theory proposed by Flores et al. [40] the distribution of LNAPL and water saturation can be determined by solving the essential matrices of the 2D tank domain using MATLAB. Figure 4 depicts the flowchart of the SIAM procedures.

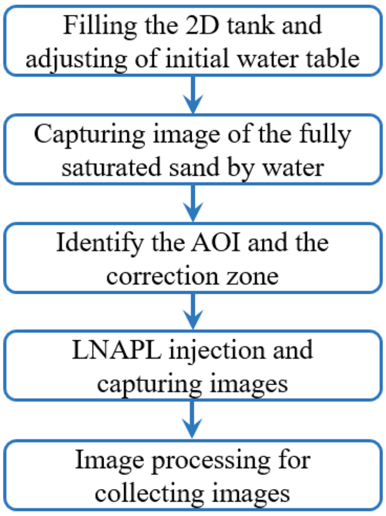

Figure 4. Flowchart of SIAM procedures

3. Results and Discussion

The LNAPL and water migration behavior is determined using SIAM after running the MATLAB code. The area of interest (AOI) was assigned to be 8 cm x 8 cm, centered on the LNAPL injection point, and intercepted for quantitative analysis. After injecting the diesel, it migrates downward in the soil pore spaces due to the effect of gravitational force. The impact of single and repetitive injections of LNAPL volume under dynamic groundwater conditions is analyzed and discussed in the next sections.

3.1. LNAPL and Water Saturation Profiles

The LNAPL and water saturation profiles of experiments with four and two intermittent injections, where the 800 ml LNAPL is injected in four and two injection stages, respectively, are illustrated in Figures 5 and 6. The 800 ml LNAPL injected in one stage is shown in Figure 7. Each injection stage is labeled as per the injected volume and the injection sequence, where the first number denotes the LNAPL injected volume, the alphabet R represents the (repetitive) case, and the last number represents the number of injection stages. For example, case 200R2 represents a 200 ml LNAPL injection repeated two times. The red and blue colors represent the LNAPL and water saturation distributions, respectively. As the LNAPL and water saturations decrease, their corresponding colors fade and vice versa. The first LNAPL injection started at t=21 hours. After injection, the LNAPL pushed the water from the soil pore spaces, and it can be seen clearly during the drainage stages where the LNAPL and water saturation profiles act inversely. During the drainage stage, the LNAPL migrated downward, and the water over the wet front edge dropped, whereas it raised again and pushed the LNAPL towards the surface during the imbibition stage. This observation is in agreement with the findings of He et al. [3], who studied the effect of initial water table height, the intensity of water table fluctuation, and the repetitive fluctuation on LNAPL behavior in a 2D tank of 50 cm (length) × 50 cm (height) × 5 cm (thickness) using the SIAM technique. In their study, they investigated the effect of dynamic groundwater on the redistribution and the shape of the LNAPL by detecting the morphological changes at each stage. The reported results showed that the groundwater fluctuation sequence has a significant influence on the redistribution of the contaminant plume. When the water table is reduced, the LNAPL plume vertical extension is developed, whereas LNAPL upward movement is enhanced after raising the water table in case of imbibition. This shows the impact of groundwater fluctuation on the LNAPL redistribution. The aforementioned study considered the repetitive groundwater fluctuation for LNAPL volume of 10 ml, whereas the current study considered the repetitive LNAPL with repetitive groundwater table fluctuation for larger LNAPL volumes of 200, 400, and 800 ml.

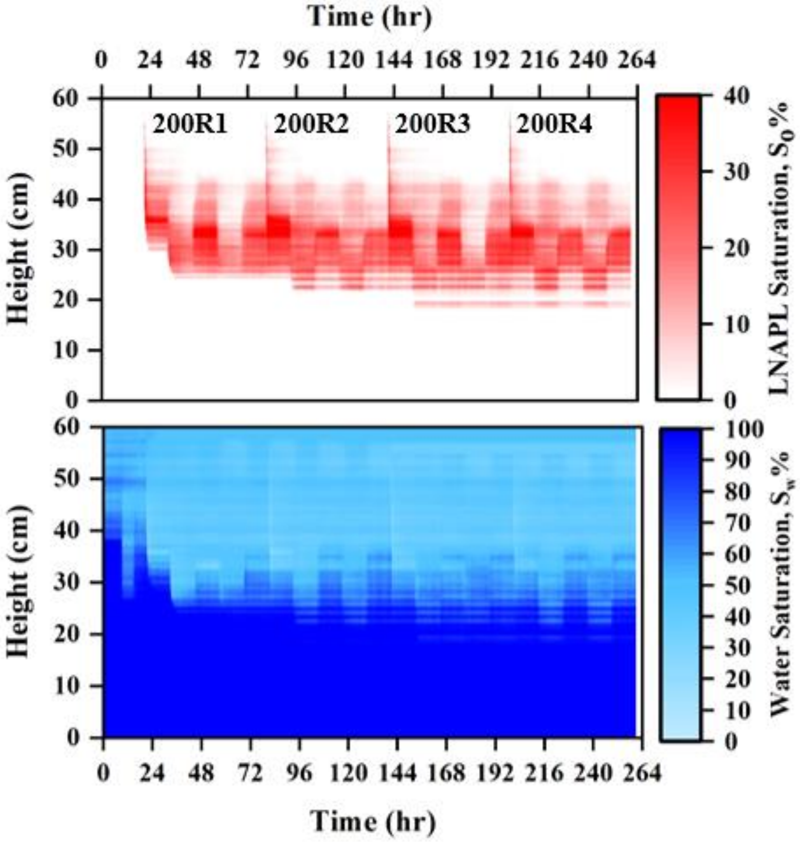

Figure 5. LNAPL and water saturation profile of case of V=800 ml in four injections

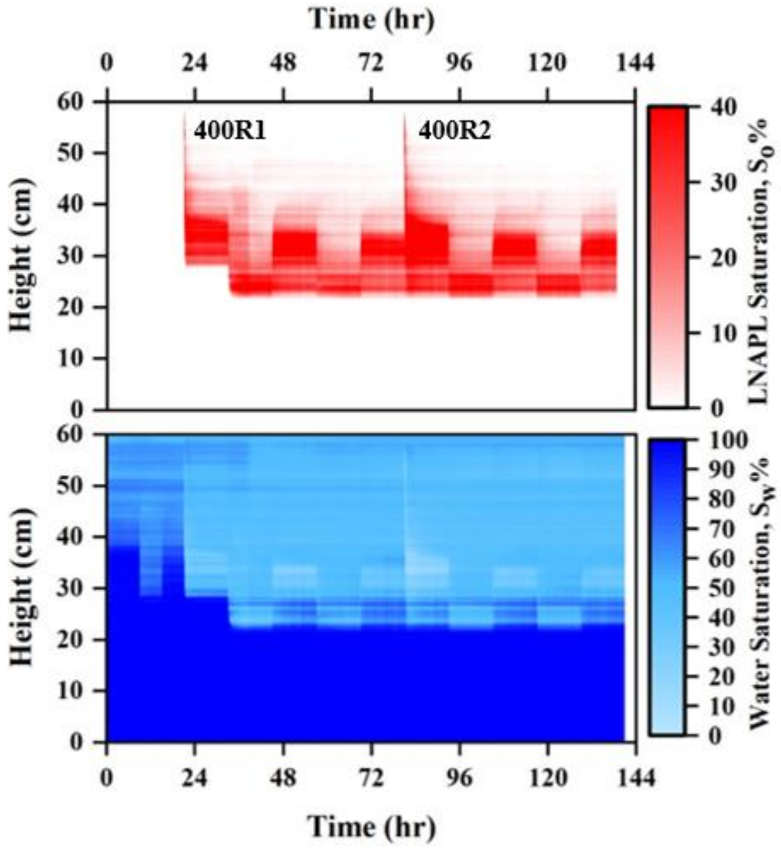

Figure 6. LNAPL and water saturation profile of case of V=800 ml in two injections

During the drainage and imbibition stages, part of the migrated LNAPL was entrapped near the wet front. This explains the entrapped dark red colour between h=18 cm and h=28 cm (from the tank bottom) at the imbibition stage when the water was raised to the height of h=28 cm as shown in Figures 5 to 7. By reducing the water table from 28 cm to 18 cm high, the mobile LNAPL migrated downward, leaving some residual LNAPL behind in the pore spaces. Consequently, this enhances the reduction in LNAPL saturation above the water table and reduces the thickness of the mobile LNAPL fraction as presented by Lenhard et al. [38]. In the study of Lenhard et al. [38], an analytical approach was used to predict the distribution of free, entrapped and residual LNAPL saturation at different elevations under equilibrium conditions. The clay loam and loamy sand were used as porous media while considering the historic effects of water table fluctuation in wells and showed that the porous media has a significant influence on the LNAPL thickness. Moreover, when the water table is increased, the water will imbibe and submerge in the smear zone (the zone of water table fluctuation). The mobile fraction of LNAPL will rise into the previous zone with residual LNAPL, enhancing the trapped LNAPL below the water table. The LNAPL interaction with the soil and the effect of one-time injection versus intermittent injections are discussed in the next sections for two overall volumes of 400 ml and 800 ml.

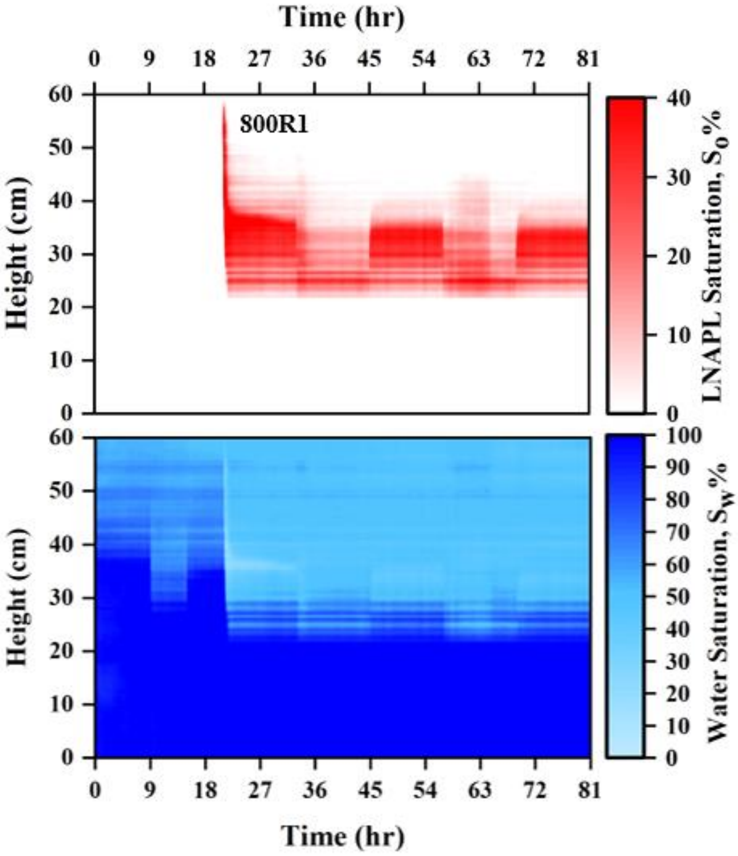

Figure 7. LNAPL and water saturation profile of case of V=800 ml in one injection

3.2. Repetitive LNAPL Injection of 400 ml

The profile of the last drainage and imbibition stages for V=400 ml LNAPL in case 200R2 of two intermittent injections and case 400R1 of one injection is shown in Figure 8. The findings are presented and analyzed concerning the transient saturations at three specific locations: the capillary fringe (h=33 cm), the highest water table (h=28 cm), and the lowest water table (h=18 cm). The LNAPL saturation of the drainage stage for 200R2 at h=28 cm and h=33 cm is 22% and 18%, respectively, as shown in Figure 9(a). In the imbibition stage, the LNAPL saturation of 200R2 (two LNAPL injections each of 200 ml) attained 19% and 27% for h=28 cm and h=33 cm, respectively. On the other hand, the LNAPL saturation of the 400R1 (one LNAPL injection of 400 ml) case at the drainage stage is 20% and 14% for h=28 cm and h=33 cm, respectively. Similarly, the LNAPL saturation of the 400R1 at the imbibition stage for h=28 cm and h=33 cm is 23% and 32%, respectively, as shown in Figure 8(b) and Figure 9(b). Intuitively, case 200R2 of double injections exhibits a superior LNAPL saturation at the drainage stage, whereas case 400R1 attains superior LNAPL saturation at the imbibition stage. At the drainage stage, Figure 8 shows that the LNAPL saturation of case 200R2 is more evenly distributed over the height of 22-42 cm compared to the case of 400R1, where the LNAPL migrated downward below the height of h=28 cm (drainage stage).

The LNAPL saturation profiles in Figures 8(a) and (b) reveal that the LNAPL is more evenly distributed through the tank height in the case of intermittent injections (200R2) compared to the case of one-time injection (400R1), characterized by larger vertical LNAPL migration and less uniform LNAPL distribution through the tank height. This observation is in agreement with Alazaiza et al. [34], who studied the LNAPL distribution of two LNAPL volumes of V=25 and 50 ml under groundwater fluctuation in a 1D column using the SIAM technique. The experimental findings showed that when the water table level was reduced from 28 cm to 18 cm high (drainage) and returned to 28 cm high (imbibition), the LNAPL saturation increased, accounting for 7% to 25%. At the drainage stage where the water is lowered from 28 cm to 18 cm high, the LNAPL saturation decreases due to its downward movement with the drained water. However, when the injected LNAPL volume is doubled to 50 ml, the LNAPL saturation at the wet front edge increases, which reflects larger subsurface groundwater contamination. Overall, both LNAPL volumes showed similar LNAPL downward migration and behavior despite the larger LNAPL saturation at the wet front edge in the case of higher volume that pushes the water downward to occupy the soil pore spaces. Alazaiza et al. [34] reported that the SIAM method is considered an economically accurate method for tracking the water and LNAPL time-dependent movement.

The LNAPL injection in 400R1 enhances the LNAPL migration to depths closer to the water table level, and therefore, 400R1 experiences larger LNAPL saturation at deeper tank heights below h=28 cm (case of drainage as an example). Similarly, this explains the larger LNAPL saturation of 200R2 at h=28 cm and h=33 cm of the drainage stage because the LNAPL of 400R1 migrates more downward and consequently, it is concentrated more below h=28 cm. Moreover, the capillary resistance, which opposes the gravitational force of the injected volume, is weaker to the gravitational force when the volume is injected at one time (larger LNAPL mass and larger gravitational force) compared to the intermittent injection (case of 200R2). The weaker capillary force in the case of 400R1 allowed larger volumes of LNAPL to migrate deeper and form larger LNAPL-saturated areas below h=28 cm at the drainage stage and in the vicinity of the wet front in the imbibition stage. This observation is attributed to the high spilled LNAPL volume that occupies a larger part of the pore spaces and forces the LNAPL to migrate further downward [37]. In the study of Alazaiza et al. [37], three different LNAPL volumes of 50, 100, and 150 ml were experimentally studied in a 1D column under precipitation. Results showed that as the LNAPL volume increases, LNAPL migrates downward faster due to the higher LNAPL pressure, which allows the migrating LNAPL to reach deeper depths in a shorter time. The same concept can be applied to the current study, where the single LNAPL injection has a larger volume pressure, which helps the LNAPL to migrate deeper and fill the soil pore spaces at a faster rate compared to the relatively lower LNAPL volume in the case of intermittent injections.

During the imbibition stage, the water level is raised from h=18 cm to h=28 cm, and therefore, the water capillary force exerts pressure on the LNAPL filled in the pore spaces and pushes the LNAPL upwards towards the surface. The capillary force is developed from the surface tension of the water molecules and sand surface. During imbibition, the surface tension pulls the water into the pores, which increases the capillary force and therefore displaces the LNAPL from the soil pore spaces upwards towards the surface. In smaller pore spaces, the capillary force is stronger, and therefore, the water will fill these areas first and displace LNAPL into larger pore spaces or towards the surface due to LNAPL's relatively lower density than water. From Figures 8 and 9, the effect of the capillary force on the LNAPL redistribution in the imbibition stage is more influential in the case of 200R2 than in the case of 400R1 due to the relatively weaker gravitational force in 200R2, which makes it more vulnerable to LNAPL redistribution under the developed capillary force.

Moreover, the LNAPL saturation in the wet front area is larger in the case of 400R1, as the LNAPL one-time injection weakens the capillary force and increases the LNAPL saturation in the soil pore spaces in the wet front vicinity. This finding agrees with Alden et al. [45], who revealed that when the groundwater table rises, a portion of the LNAPL moves upwards, while part of the contaminant becomes entrapped by water due to the effect of capillary forces. The LNAPL saturation may increase and become trapped below the water table in the saturated zone, depending on the water level differences during fluctuation. As the LNAPL migrates in the unsaturated soil, residual LNAPL can be retained in the encountered pore spaces. On the other hand, the LNAPL upward redistribution of case 200R2 is larger (LNAPL redistribution between h=28 cm and h=33 cm) due to its weaker resistance against the exerted capillary force. Overall, the comparison between injecting V=400 ml at a one-time injection (case of 400R1) or through two injections (case of 200R2) shows that when the volume is injected in one stage, the LNAPL redistribution is weaker near the tank surface, whereas it is larger and more concentrated at larger depths near the wet front. Moreover, the one-time injection causes a larger volume of LNAPL to migrate downward to the wet front area and increases the entrapped LNAPL at that depth. This raises additional risks of subsurface underground water table contamination and challenges researchers, authorities, and experts in understanding the LNAPL behavior at deeper levels and mitigating further environmental or ecological damages through enforcing the right remediation measures.

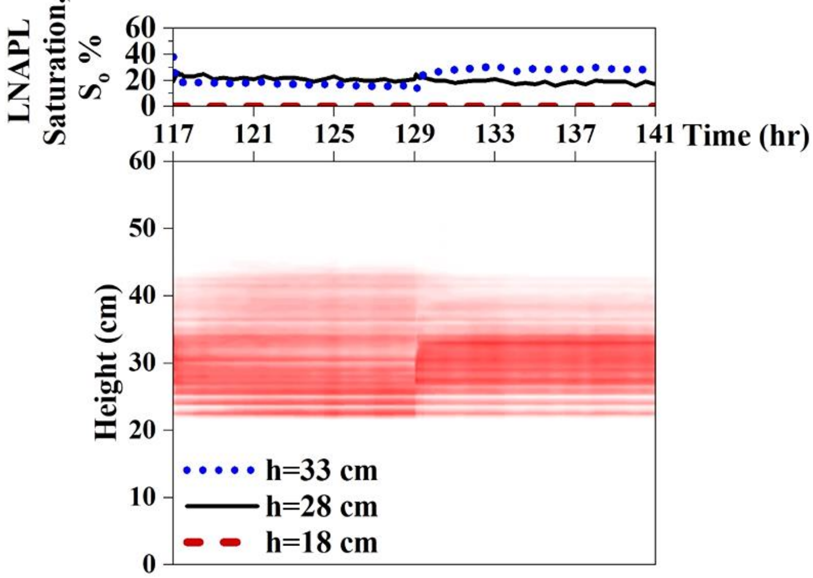

a)

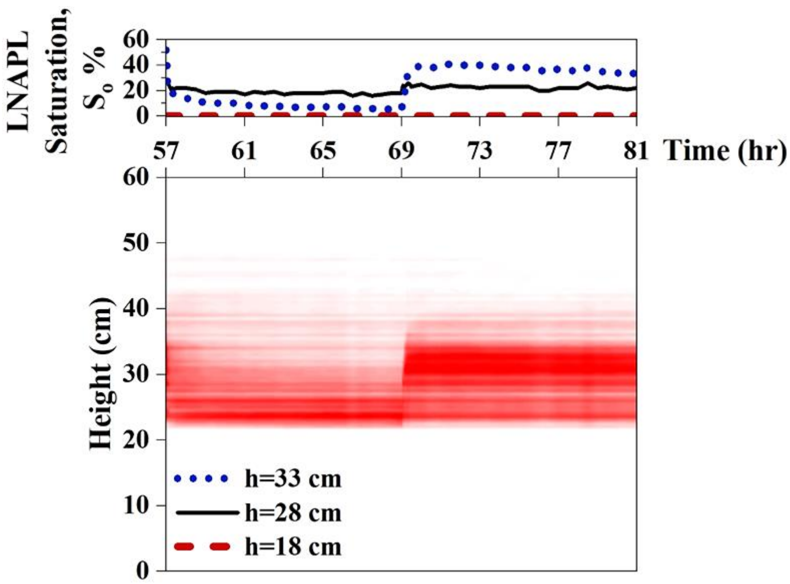

b)

Figure 8. LNAPL saturation profile of last drainage and imbibition stages: a) 200R2 and b) 400R1

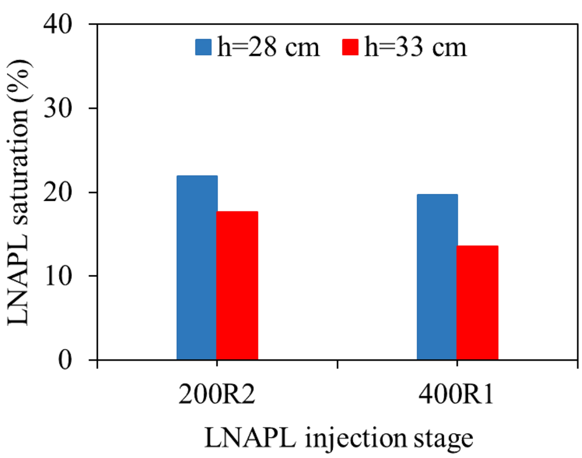

a)

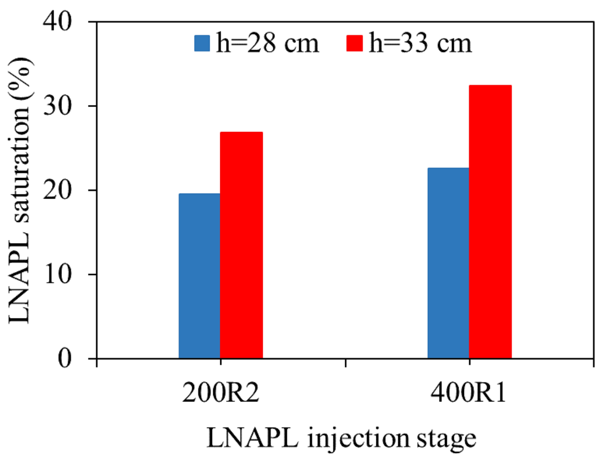

b)

Figure 9. LNAPL average saturation of 200R2 and 400R1: a) last drainage and b) last imbibition

3.3. Repetitive LNAPL Injection of 800 ml

In this section, the effect of injecting LNAPL through one or intermittent injections is investigated for a total LNAPL volume of 800 ml. Figure 10 depicts the LNAPL saturation profiles for the last drainage and imbibition of the cases 200R4 (four LNAPL injections each of 200 ml), 400R2 (two LNAPL injections each of 400 ml), and 800R1 (one LNAPL injection of 800 ml). Similarly, Figure 11 illustrates the LNAPL average saturation for the cases of 200R4, 400R2, and 800R1 at h=28 cm and 33 cm from the tank bottom. The LNAPL saturation of the drainage stage for 200R4 at h=28 cm and h=33 cm is 20% and 15%, respectively, as shown in Figure 11-a. In the imbibition stage, the LNAPL saturation in the case of 200R4 attained 24% and 30% for h=28 cm and h=33 cm, respectively. However, LNAPL saturation in the case of 400R2 at the drainage stage is 18% and 9% at the higher water table (h=28 cm) and the capillary fringe zone (h=33 cm), respectively. Similarly, the LNAPL saturation of the imbibition stage of the 400R2 is 23% and 34% for h=28 cm and h=33 cm, respectively, as shown in Figures 10-b and 11-b. In the case of 800R1, where the LNAPL spilled one time, the LNAPL saturation of the drainage stage is 24% and 17% at h=28 cm and h=33 cm, respectively. This saturation increased in the imbibition stage when the water table increased from h=18 cm to h=28 cm to be 28% and 36% at h=28 cm and h=33 cm, respectively, as shown in Figures١٠-c and 11-c. In the three cases, the LNAPL did not cross the wet front threshold of h=18 cm.

Unlike the cases of 400R2 and 800R1, the LNAPL of 200R4 (four injections) migrated deeper to the wet front edge of h=18.5 cm for both drainage and imbibition cycles. This can be attributed to the effect of repetitive groundwater table fluctuation in the case of 200R4 (subjected to a larger number of drainage and imbibition cycles than the cases of 400R2 and 800R1). During LNAPL infiltration, the LNAPL migrates downward to fill preferential paths. However, as the LNAPL volume increases, it gains the ability to diffuse from the preferential paths to small pore spaces of the soil. Therefore, LNAPL vertical infiltration can increase specifically under water table fluctuations (drainage/imbibition). When the LNAPL volume is sufficient, it can migrate from preferential paths into smaller pore spaces of the soil matrix, specifically under the drainage-imbibition underground water conditions. This is attributed to larger pressure and gravitational force for larger LNAPL volumes, which helps the LNAPL to overcome the capillary force and move to occupy smaller soil pore spaces. The preferential paths of soil are formed by relatively large interconnected pores, which allow LNAPL to move more freely through these paths with lower energy to traverse. For small LNAPL volume, it moves in the easiest path, known as the preferential path, usually characterized by relatively larger pores where capillary force is lower. When volume increases, LNAPL fills the pore spaces and starts spreading into adjacent smaller pore spaces under the effect of volume pressure and gravitational force until the LNAPL exceeds the capillary force that prevents its movement into finer pores. Moreover, the LNAPL distribution in the case 200R4 (V=800 ml) exhibits a similar pattern to the case of 200R2 (V=400 ml), as both show a more evenly distributed LNAPL saturation profile through the tank depth than the cases of 800R1 and 400R2, respectively. This observation is clearer as the height increases towards the surface. On the other hand, the LNAPL saturation of cases 800R1 and 400R2 is larger for h<28 cm. A higher vertical contaminant diffusion caused by the effect of gravity makes the LNAPL predominantly migrate downward at a faster rate when the spilled volume is high, as stated by Yang et al. [46].

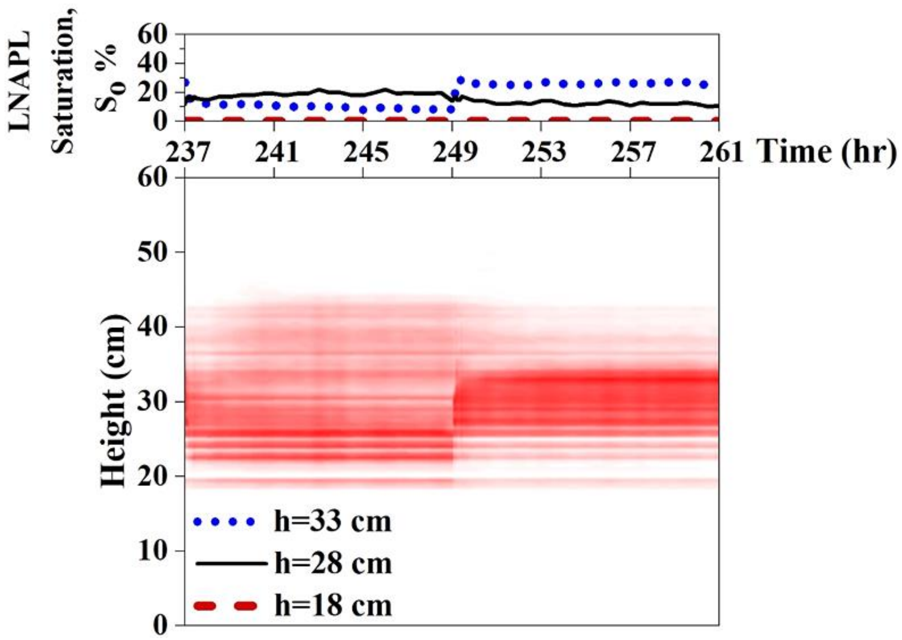

a)

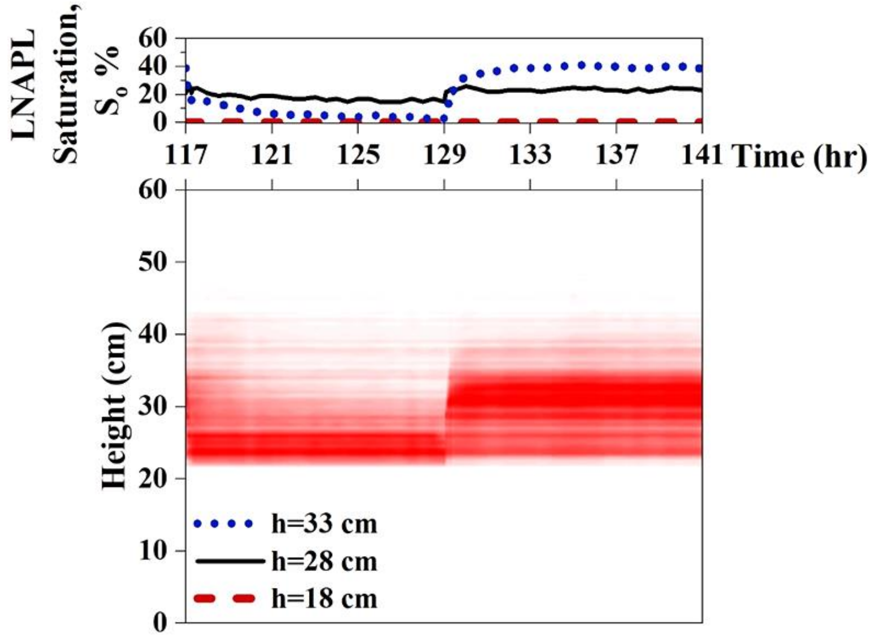

b)

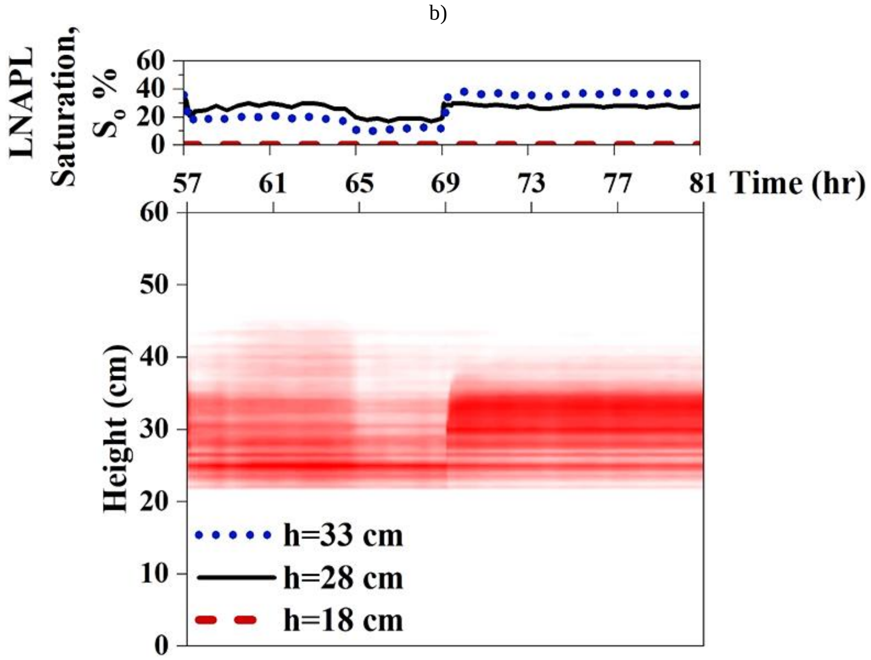

c)

Figure 10. LNAPL saturation profile of the last drainage and imbibition stages: a) 200R4; b) 400R2 and c) 800R1

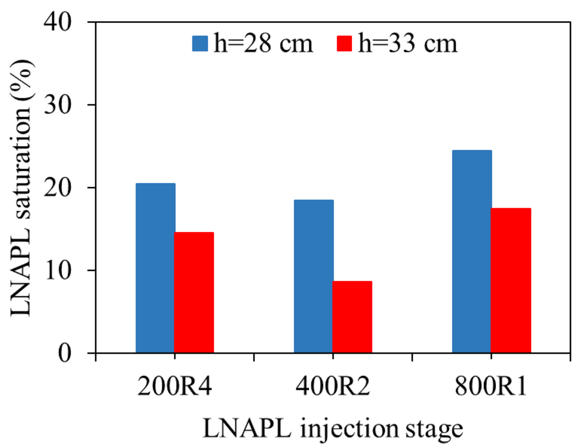

a)

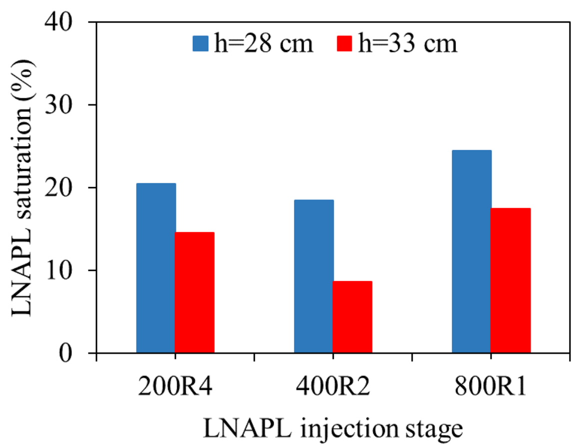

b)

Figure 11. LNAPL average saturation of 200R4, 400R2 and 800R1: a) last drainage and b) last imbibition

During the drainage stage, the larger volume injected at one stage (800R1) (Figure 10-c) acquires a larger gravitational force (gravitational force (F)= LNAPL mass (m)×gravitational acceleration(g)) that pushes the LNAPL to migrate downward and fill the pore spaces between h=18 cm and h=28 cm. Intuitively, the larger LNAPL injected volume at once has a larger resistance against the capillary force of the imbibition stage when the water level is raised from h=18 cm to h=28 cm. Therefore, the LNAPL saturation is larger in the case of 800R1 than in the cases of 400R2 and 200R4. In the cases of 800R1 and 400R2 where the capillary force is weaker against their larger injected volume and therefore, more LNAPL is entrapped below the imbibition water level of h=28 cm as shown in Figures 10 and 11-a. This is related to the reduction in the LNAPL permeability with increasing moisture content, which decreases the LNAPL flux [47, 48]. Moreover, the case of 800R1 exhibits a larger LNAPL saturation in the vicinity of the wet front level (at h=28 cm) than the cases of 400R2 and 200R4 as shown in Figure 11. In partially saturated soil (soil pores contain both water and air), LNAPL generally migrates through larger air-filled pore spaces which act as preferential flow paths and allow high LNAPL flux (rate of flow). For LNAPL to migrate downwards, it must overcome the capillary forces and flow through pores that are not occupied by water. Therefore, higher LNAPL permeability indicates more free movement and lower LNAPL permeability hinders LNAPL flow. When the soil moisture content increases, LNAPL permeability through soil is reduced due to lighter LNAPL density to water, and consequently, the LNAPL flux is reduced.

The smaller intermittent injection stage of 200 ml in 200R4 has a weaker gravitational force to oppose the initiated capillary force of the imbibition stage and consequently, the water pushed the LNAPL from the deep pore spaces to the area above the wet front of h=28 cm as shown in Figure 10(a). For instance, the LNAPL saturation at the imbibition and drainage stages for h=28 cm and h=33 cm is higher in 800R1 than the cases of intermittent injections (400R2 and 200R1) due to the larger LNAPL volume injected in one stage which enhanced the downward LNAPL movement. On the other hand, Figure 11 shows that the LNAPL saturation of the drainage stage for the case of 200R4 is larger than the case of 400R2 for both sections of h=28 cm and h=33 cm. This is explained by greater LNAPL penetration at the drainage stage of the case of 400R2 which reduced the LNAPL saturation at h=28 cm and h=33 cm and increased its saturation for the area of h<28 cm. The larger LNAPL volume of each injection in the case of 400R2 compared to the case of 200R4 increased its saturation and distribution below h=28 cm due to its larger gravitational force compared to the case of 200R4 which has a weaker potential against the capillary force specifically at deeper heights (h<28 cm).

Overall, the capillary force, which resists the LNAPL movement in the soil, depends on several parameters such as the pore size, soil LNAPL saturation, and LNAPL surface tension. The gravitational force that pulls the LNAPL downward through the soil is proportional to the mass/volume of the injected LNAPL. In the current study, there are two LNAPL injection scenarios. In the first scenario, LNAPL is injected through smaller doses where its dose has less mass than the one-dose injection, which indicates a lower gravitational force of each injection that permits the capillary force to mitigate the LNAPL downward movement. This is attributed to the relatively stronger capillary force each injected dose encountered with respect to its gravitational force, which hinders its downward migration through the soil. Over time, this is reflected by less deep LNAPL distribution for the case of intermittent smaller injections compared to the case of a one-time injection of the same overall volume. In the second scenario of one-time LNAPL injection, the LNAPL of larger mass has a higher gravitational force, which pushes the LNAPL downward to overcome the capillary force more efficiently.

The capillary force depends on the surface tension between water molecules and the sand surface. Consequently, for larger LNAPL mass injected at one time, which has a relatively larger gravitational force compared to the case of LNAPL intermittent injections with smaller masses, LNAPL is more capable of overcoming the capillary force and migrating downward towards the wet front edge. The redistribution of LNAPL saturation through the soil depths is governed by the balance of the capillary force and the gravitational force. This balance is crucial in subsurface soil and groundwater contamination as it has a significant influence on the LNAPL movement and distribution as well as remediation strategies. Larger LNAPL injections, such as the case of one-time injection, can lead to deeper LNAPL movement and raise the threat of groundwater contamination. However, understanding the effect of the injected LNAPL volume and repetitive injections can help to improve the remediation controlling methods and reduce the contamination extent. The results of this study aim to provide a fundamental understanding that can be applied to larger-scale site studies and model predictions rather than a direct simulation of field natural conditions. Understanding these concepts improves applying the findings of this study to real-world scenarios while identifying the lab setup limitations.

4. Conclusions

LNAPL leaking in the subsurface systems is an ongoing environmental problem due to the potential risks of groundwater contamination to receptors. Understanding the influence of single and repetitive LNAPL spills in a system subjected to groundwater table fluctuation on the transient evolution of LNAPL is necessary for accurate remediation efforts. This study conducted controlled experiments using a 2D tank of 70 cm × 70 cm × 3.5 cm to evaluate the influence of single and intermittent LNAPL spills under dynamic groundwater conditions on LNAPL migration and saturation. The tank was filled with river sand as a porous medium of particle size ranging from 0.15 mm to 2 mm. The LNAPL and water saturation profiles in the entire domain of the 2D tank under dynamic groundwater conditions were provided using SIAM. Single and intermittent LNAPL (diesel) spills of a total volume of 400 ml and 800 ml were tested in this study to assess LNAPL migration under the influence of groundwater table fluctuation.

The intermittent injection for total LNAPL volume of 400 and 800 ml showed that the LNAPL saturation was redistributed more evenly through the tank height in the case of intermittent injections compared to the case of one-time injection. Whereas the LNAPL saturation distribution is oriented to migrate deeper to the wet front area at larger rates in the case of one-time injection enhanced by its larger gravitational force and weaker capillary force. Consequently, LNAPL entrapment is more pronounced in the case of one-time injection. Overall, the comparison between injecting V=400 ml at a one-time injection (case of 400R1) or through two injections (case of 200R2) shows that when the volume is injected in one stage, the LNAPL redistribution is weaker near the tank surface, whereas it is larger and more concentrated at larger depths near the wet front. Moreover, the one-time injection enhances LNAPL migration to the wet front area and raises additional risks of subsurface underground water table contamination.

The range of LNAPL distribution through the tank height showed a similar pattern in all cases of tested experiments. Despite the similar range of LNAPL distribution, the LNAPL saturation of intermittent injections at deeper levels is lower than the one-time injection and vice versa at higher levels of the tank. When the LNAPL overall volume is 400 ml, the LNAPL distribution is above h=28 cm high, whereas LNAPL migrated below h=28 cm when the overall LNAPL injected volume is raised to 800 ml with the highest saturation of 36%. As the total injected volume increases, the LNAPL saturation at deeper levels is larger, and larger LNAPL entrapment is exhibited, which raises concerns about larger groundwater contamination and more severe damage to human health, the ecosystem, and the environment. The LNAPL saturation in the case 200R4 is more evenly distributed through the tank depth than in the cases of 800R1 and 400R2. The smaller intermittent injection stage of 200 ml in 200R4 has a weaker gravitational force and stronger capillary force, and consequently, the water pushed the LNAPL from the deep pore spaces to the area above the wet front of h=28 cm during the imbibition stage. The LNAPL saturation of the drainage stage for the case of 200R4 is larger than the case of 400R2 for both sections of h=28 cm and h=33 cm. This is explained by greater LNAPL penetration at the drainage stage of the case of 400R2, which reduced the LNAPL saturation at h=28 cm and h=33 cm and increased its saturation for the area of h<28 cm.

Overall, this study showed that repetitive LNAPL spills pose severe risks to the environment, especially when combined with water table fluctuation. It was shown that even with a small injected volume, the LNAPL can migrate deeper close to the saturated zone due to fluctuation in the water table. Therefore, it is important to consider the effect of dynamic groundwater conditions when determining the effects of other parameters on LNAPL migration, such as single and repetitive LNAPL spills. Based on the findings from this study, practical implications of the LNAPL spill monitoring system and post-spill management strategy were proposed. Once the spill occurs, fast action should be taken into consideration, such as covering the limits of the contaminated site to prevent further migration of the contaminant into the groundwater. The study also showed that the SIAM technique, which relies on light intensity variations, is an effective and simple tool to allow accurate visualization of the water table fluctuation on the transient LNAPL migration. This work produced comprehensive results for various LNAPL spills migrating under dynamic groundwater conditions, which provide a sound basis for future studies.

5. Declarations

5.1. Author Contributions

Conceptualization, D.F.A.; methodology, D.F.A.; software, D.F.A.; validation, D.F.A.; formal analysis, D.F.A.; data curation, D.F.A; writing—original draft preparation, D.F.A.; writing—review and editing, D.F.A., H.R., and A.Z.; visualization, D.F.A., H.R., and A.Z.; supervision, D.F.A., H.R., and A.Z.; project administration, H.R.; funding acquisition, H.R. All authors have read and agreed to the published version of the manuscript.

5.2. Data Availability Statement

The data presented in this study are available on request from the corresponding author.

5.3. Funding

The research is funded by the Ministry of Higher Education Malaysia under the Fundamental Research Grant Scheme with grant number FRGS/1/2018/TK01/USM/03/4.

5.4. Acknowledgements

The authors wish to express sincere appreciation for the support from Universiti Sains Malaysia in making this project a success. The authors also gratefully acknowledge the financial support provided by the Southern Technical University Iraq and the Ministry of Higher Education Malaysia.

5.5. Conflicts of Interest

The authors declare no conflict of interest.

6. References

[1] Vuruna, M., Veličković, Z., Perić, S., Bogdanov, J., Ivanković, N., & Bučko, M. (2017). The influence of atmospheric conditions on the migration of diesel fuel spilled in soil. Archives of Environmental Protection, 43(1), 73–79. doi:10.1515/aep-2017-0004.

[2] Maire, J., Joubert, A., Kaifas, D., Invernizzi, T., Marduel, J., Colombano, S., Cazaux, D., Marion, C., Klein, P. Y., Dumestre, A., & Fatin-Rouge, N. (2018). Assessment of flushing methods for the removal of heavy chlorinated compounds DNAPL in an alluvial aquifer. Science of the Total Environment, 612, 1149–1158. doi:10.1016/j.scitotenv.2017.08.309.

[3] He, Z., Liang, F., Meng, J., & Li, N. (2022). Effects of groundwater fluctuation on migration characteristics and representative elementary volume of entrapped LNAPL. Journal of Hydrology, 610. doi:10.1016/j.jhydrol.2022.127833.

[4] Newell, C. J., Acree, S. D., Ross, R. R., & Huling, S. G. (1995). Ground Water Issue. United States Environmental Protection Agency, EPA/540/S-95/500.

[5] Luciano, A., Viotti, P., & Papini, M. P. (2010). Laboratory investigation of DNAPL migration in porous media. Journal of Hazardous Materials, 176(1–3), 1006–1017. doi:10.1016/j.jhazmat.2009.11.141.

[6] Agaoglu, B., Copty, N. K., Scheytt, T., & Hinkelmann, R. (2015). Interphase mass transfer between fluids in subsurface formations: A review. Advances in Water Resources, 79, 162–194. doi:10.1016/j.advwatres.2015.02.009.

[7] Dalhat, M. N. (2005). Effect of rate of water table rise on LNAPL entrapment in uniform and well-graded sands. Ph.D. Thesis, King Fahd University of Petroleum and Minerals, Dhahran, Saudi Arabia.

[8] Dobson, R., Schroth, M. H., & Zeyer, J. (2007). Effect of water-table fluctuation on dissolution and biodegradation of a multi-component, light nonaqueous-phase liquid. Journal of Contaminant Hydrology, 94(3–4), 235–248. doi:10.1016/j.jconhyd.2007.07.007.

[9] Gomo, M. (2009). Site characterisation of LNAPL-contaminated fractured-rock aquifer. Ph.D. Thesis, University of the Free State, Bloemfontein, South Africa.

[10] Cavelan, A., Golfier, F., Colombano, S., Davarzani, H., Deparis, J., & Faure, P. (2022). A critical review of the influence of groundwater level fluctuations and temperature on LNAPL contaminations in the context of climate change. Science of the Total Environment, 806. doi:10.1016/j.scitotenv.2021.150412.

[11] Alazaiza, M. Y. D., Ngien, S. K., Bob, M. M., Kamaruddin, S. A., & Ishak, W. M. F. (2018). Non-aqueous phase liquids distribution in three-fluid phase systems in double-porosity soil media: Experimental investigation using image analysis. Groundwater for Sustainable Development, 7, 133–142. doi:10.1016/j.gsd.2018.04.002.

[12] Jiang, W., Yang, J., Zhu, J., Liu, Y., Chen, Y., Sun, Q., Wang, Y., & Zhang, H. (2018). Experimental study on the transport characteristics of buried pipeline leakage and the performance of groundwater remediation system. Environmental Science and Pollution Research, 25(36), 36570–36580. doi:10.1007/s11356-018-3490-0.

[13] Yang, Z. H., Verpoort, F., Dong, C. Di, Chen, C. W., Chen, S., & Kao, C. M. (2020). Remediation of petroleum-hydrocarbon contaminated groundwater using optimized in situ chemical oxidation system: Batch and column studies. Process Safety and Environmental Protection, 138, 18–26. doi:10.1016/j.psep.2020.02.032.

[14] Belfort, B., Weill, S., Fahs, M., & Lehmann, F. (2019). Laboratory experiments of drainage, imbibition and infiltration under artificial rainfall characterized by image analysis method and numerical simulations. Water (Switzerland), 11(11), 2232. doi:10.3390/w11112232.

[15] Smith, J. W. N., Davis, G. B., Devaull, G. E., Garg, S., Newell, C. J., & Rivett, M. O. (2022). Natural Source Zone Depletion (NSZD): from process understanding to effective implementation at LNAPL-impacted sites. Quarterly Journal of Engineering Geology and Hydrogeology, 55(4), 1-10. doi:10.1144/qjegh2021-166.

[16] Haberer, C. M., Rolle, M., Cirpka, O. A., & Grathwohl, P. (2012). Oxygen Transfer in a Fluctuating Capillary Fringe. Vadose Zone Journal, 11(3), 56. doi:10.2136/vzj2011.0056.

[17] Mahmoudi, D., Rezaei, M., Ashjari, J., Salehghamari, E., Jazaei, F., & Babakhani, P. (2020). Impacts of stratigraphic heterogeneity and release pathway on the transport of bacterial cells in porous media. Science of the Total Environment, 729, 138804. doi:10.1016/j.scitotenv.2020.138804.

[18] Mineo, S. (2023). Groundwater and soil contamination by LNAPL: State of the art and future challenges. Science of The Total Environment, 874, 162394. doi:10.1016/j.scitotenv.2023.162394.

[19] Zaiter, A., Sabtu, N., & Almaliki, D. F. (2024). Equations and methodologies of inlet drainage system discharge coefficients: A review. Open Engineering, 14(1), 20220598. doi:10.1515/eng-2022-0598.

[20] Fetter, C. W., Boving, T., & Kreamer, D. (2017). Contaminant hydrogeology. Waveland Press, Long Grove, United States.

[21] Huang, X., Liu, G., Xia, C., & Yang, M. (2021). Simulated groundwater dynamics and solute transport in a coastal phreatic aquifer subjected to different tides. Marine Georesources and Geotechnology, 39(6), 719–734. doi:10.1080/1064119X.2020.1754975.

[22] Koohbor, B., Colombano, S., Harrouet, T., Deparis, J., Lion, F., Davarzani, D., & Ataie-Ashtiani, B. (2023). The effects of water table fluctuation on LNAPL deposit in highly permeable porous media: A coupled numerical and experimental study. Journal of Contaminant Hydrology, 256. doi:10.1016/j.jconhyd.2023.104183.

[23] Williams, M. D., & Oostrom, M. (2000). Oxygenation of anoxic water in a fluctuating water table system: An experimental and numerical study. Journal of Hydrology, 230(1–2), 70–85. doi:10.1016/S0022-1694(00)00172-4.

[24] Lenhard, R. J., Oostrom, M., & Dane, J. H. (2004). A constitutive model for air–NAPL–water flow in the vadose zone accounting for immobile, non-occluded (residual) NAPL in strongly water-wet porous media. Journal of Contaminant Hydrology, 73(1–4), 283–304. doi:10.1016/j.jconhyd.2004.07.005.

[25] Alazaiza, M. Y. D., Ngien, S. K., Copty, N., Bob, M. M., & Kamaruddin, S. A. (2019). Assessing the influence of infiltration on the migration of light non-aqueous phase liquid in double-porosity soil media using a light transmission visualization method. Hydrogeology Journal, 27(2), 581–593. doi:10.1007/s10040-018-1904-1.

[26] Gupta, P. K., Yadav, B., & Yadav, B. K. (2019). Assessment of LNAPL in Subsurface under Fluctuating Groundwater Table Using 2D Sand Tank Experiments. Journal of Environmental Engineering, 145(9), 1–13. doi:10.1061/(asce)ee.1943-7870.0001560.

[27] Almaliki, D. F., & Ramli, H. (2024). A Review on Simplified Image Analysis Method for Measuring LNAPL Saturation Under Groundwater Table Fluctuation. Lecture Notes in Civil Engineering, 386, 93–108. doi:10.1007/978-981-99-6026-2_8.

[28] Ramli, M. H. B. (2014). Dynamic effects on migration of light non-aqueous phase liquids in subsurface. Ph.D. Thesis, Kyoto University, Kyoto, Japan.

[29] Qi, S., Luo, J., O'Connor, D., Wang, Y., & Hou, D. (2020). A numerical model to optimize LNAPL remediation by multi-phase extraction. Science of the Total Environment, 718, 137309. doi:10.1016/j.scitotenv.2020.137309.

[30] Shen, H., Huang, Y., Illman, W. A., Su, Y., & Miao, K. (2023). Migration behaviour of LNAPL in fractures filled with porous media: Laboratory experiments and numerical simulations. Journal of Contaminant Hydrology, 253, 104118. doi:10.1016/j.jconhyd.2022.104118.

[31] Alazaiza, M. Y. D., Copty, N. K., & Abunada, Z. (2020). Experimental investigation of cosolvent flushing of DNAPL in double-porosity soil using light transmission visualization. Journal of Hydrology, 584. doi:10.1016/j.jhydrol.2020.124659.

[32] Yimsiri, S., Euaapiwatch, S., Flores, G., Katsumi, T., & Likitlersuang, S. (2018). Effects of water table fluctuation on diesel fuel migration in one-dimensional laboratory study. European Journal of Environmental and Civil Engineering, 22(3), 359–385. doi:10.1080/19648189.2016.1197158.

[33] Van De Ven, C. J. C., Scully, K. H., Frame, M. A., Sihota, N. J., & Mayer, K. U. (2021). Impacts of water table fluctuations on actual and perceived natural source zone depletion rates. Journal of Contaminant Hydrology, 238, 103771. doi:10.1016/j.jconhyd.2021.103771.

[34] Alazaiza, M. Y. D., Ramli, M. H., Copty, N. K., Sheng, T. J., & Aburas, M. M. (2020). LNAPL saturation distribution under the influence of water table fluctuations using simplified image analysis method. Bulletin of Engineering Geology and the Environment, 79(3), 1543–1554. doi:10.1007/s10064-019-01655-3.

[35] Flores, G., Katsumi, T., Eua-Apiwatch, S., Lautua, S., & Inui, T. (2016). Migration of different LNAPLs in subsurface under groundwater fluctuating conditions by the simplified image analysis method. Journal of Geo-Engineering Sciences, 3(1), 15–30. doi:10.3233/jgs-150033.

[36] Azimi, R., Vaezihir, A., Lenhard, R. J., & Majid Hassanizadeh, S. (2020). Evaluation of LNAPL behavior in water table inter-fluctuate zone under groundwater drawdown condition. Water (Switzerland), 12(9), 2337. doi:10.3390/W12092337.

[37] Alazaiza, M. Y. D., Ramli, M. H., Copty, N. K., & Ling, M. C. (2021). Assessing the impact of water infiltration on LNAPL mobilization in sand column using simplified image analysis method. Journal of Contaminant Hydrology, 238, 103769. doi:10.1016/j.jconhyd.2021.103769.

[38] Lenhard, R. J., Rayner, J. L., & Davis, G. B. (2017). A practical tool for estimating subsurface LNAPL distributions and transmissivity using current and historical fluid levels in groundwater wells: Effects of entrapped and residual LNAPL. Journal of Contaminant Hydrology, 205, 1–11. doi:10.1016/j.jconhyd.2017.06.002.

[39] Zheng, J., Yang, Y., Li, J., Zhang, H., & Ma, Y. (2023). The Migration Mechanism of BTEX in Single- and Double-Lithology Soil Columns under Groundwater Table Fluctuation. Toxics, 11(7), 630. doi:10.3390/toxics11070630.

[40] Flores, G., Katsumi, T., Inui, T., & Kamon, M. (2011). A simplified image analysis method to study LNAPL migration in porous media. Soils and Foundations, 51(5), 835–847. doi:10.3208/sandf.51.835.

[41] Alazaiza, M. Y. D., Maskari, T. Al, Albahansawi, A., Amr, S. S. A., Abushammala, M. F. M., & Aburas, M. (2021). Diesel migration and distribution in capillary fringe using different spill volumes via image analysis. Fluids, 6(5), 189. doi:10.3390/fluids6050189.

[42] Hanlan, J., Skoog, D. A., & West, D. M. (1973). Principles of Instrumental Analysis. Studies in Conservation, 18(1), 45. doi:10.2307/1505543.

[43] Kechavarzi, C., Soga, K., & Wiart, P. (2000). Multispectral image analysis method to determine dynamic fluid saturation distribution in two-dimensional three-fluid phase flow laboratory experiments. Journal of Contaminant Hydrology, 46(3–4), 265–293. doi:10.1016/S0169-7722(00)00133-9.

[44] Bob, M. M., Brooks, M. C., Mravik, S. C., & Wood, A. L. (2008). A modified light transmission visualization method for DNAPL saturation measurements in 2-D models. Advances in Water Resources, 31(5), 727–742. doi:10.1016/j.advwatres.2008.01.016.

[45] Alden, D.F., García-Rincón, J., Rivett, M.O., Wealthall, G.P., & Thomson, N.R. (2024). Complexities of Petroleum Hydrocarbon Contaminated Sites. Advances in the Characterisation and Remediation of Sites Contaminated with Petroleum Hydrocarbons. Environmental Contamination Remediation and Management. Springer, Cham, Switzerland. doi:10.1007/978-3-031-34447-3_1.

[46] Yang, Y., Li, J., Lv, N., Wang, H., & Zhang, H. (2023). Multiphase migration and transformation of BTEX on groundwater table fluctuation in riparian petrochemical sites. Environmental Science and Pollution Research, 30(19), 55756–55767. doi:10.1007/s11356-023-26393-8.

[47] Charbeneau, R. J. (2006). Groundwater hydraulics and pollutant transport. Waveland Press, Long Grove, United States.

[48] Zuo, R., Wu, Z., Li, J., Zheng, S., Liu, J., Han, K., Liu, Y., & Wang, J. (2023). Retention effect and mode of capillary zone on the migration process of LNAPL pollutants based on experimental exploration. Ecotoxicology and Environmental Safety, 253, 114669. doi:10.1016/j.ecoenv.2023.114669.